J|A|C|S
ARTICLES
Published on Web 01/21/2006

Conductance of Single Alkanedithiols: Conduction Mechanism and Effect of Molecule−Electrode Contacts

Xiulan Li,[†] Jin He,[‡] Joshua Hihath,[†] Bingqian Xu,[†] Stuart M. Lindsay,*[,‡,§,||] and Nongjian Tao*[,†]

Contribution from the Department of Electrical Engineering and Center for Solid State Electronic Research, Biodesign Institute, Department of Physics and Astronomy, and Department of Chemistry and Biochemistry, Arizona State University, Tempe, Arizona 85287

Received November 4, 2005; E-mail: stuart.lindsay@asu.edu; nongjian.tao@asu.edu

Abstract: The conductance of single alkanedithiols covalently bound to gold electrodes has been studied by statistical analysis of repeatedly created molecular junctions. For each molecule, the conductance histogram reveals two sets of well-defined peaks, corresponding to two different conductance values. We have found that (1) both conductance values decrease exponentially with the molecular length with an identical decay constant, $\beta \approx 0.84$ Å^{-1}, but with a factor of 5 difference in the prefactor of the exponential function. (2) The current−voltage curves of the two sets can be fit with the Simmons tunneling model. (3) Both conductance values are independent of temperature (between −5 and 60 °C) and the solvent. (4) Despite the difference in the conductance, the forces required to break the molecular junctions are the same, 1.5 nN. These observations lead us to believe that the conduction mechanism in alkanedithiols is due to electron tunneling or superexchange via the bonds along the molecules, and the two sets of conductance peaks are due to two different microscopic configurations of the molecule−electrode contacts.

Introduction

The ability to measure the conductance of a single molecule is a basic requirement in molecular electronics.[1−5] To reliably measure the conductance of a molecule, one must provide a reproducible electronic coupling between the molecule and probing electrodes.[6−9] Due to the difficulty in forming microscopically identical molecule−electrode contacts, a statistical analysis of a large number of molecular junctions is necessary to obtain a complete picture. The break junction approach[10−13] is a suitable method for this purpose because it can quickly create molecular junctions with microscopically different molecule−electrode contacts. Smit et al.[13] showed that a single hydrogen molecule forms a stable bridge between platinum electrodes using mechanically controllable break junctions. Several groups used scanning tunneling microscopy (STM) to measure single-molecule conductance by repeatedly forming molecular junctions in which molecules are covalently bound to two gold electrodes.[14−19] Conductance histograms constructed from the individual measurements reveal well-defined peaks, which represent the most probable microscopic configurations of the molecular junctions. The peaks are located at integer multiples of a fundamental conductance value, which is used as the signature to identify the conductance of a single molecule. This method has been used to reproducibly determine single molecule conductance of molecules terminated with thiols.[14,15,17,20−24] Although the thiol groups can bind to Au electrodes and form a stable molecular junction, the binding

[†] Department of Electrical Engineering and Center for Solid State Electronic Research.
[‡] Biodesign Institute.
[§] Department of Physics and Astronomy.
[||] Department of Chemistry and Biochemistry.

(1) Aviram, A.; Ratner, M. A. *Chem. Phys. Lett.* **1974**, *29*, 277−283.
(2) Joachim, C.; Gimzewski, J. K.; Aviram, A. *Nature* **2000**, *408*, 541−548.
(3) Heath, J. R.; Ratner, M. A. *Phys. Today* **2003**, *56*, 43−49.
(4) Nitzan, A.; Ratner, M. A. *Science* **2003**, *300*, 1384−1389.
(5) Carroll, R. L.; Gorman, C. B. *Angew. Chem., Int. Ed.* **2002**, *41*, 4379−4399.
(6) Cui, X. D.; Primak, A.; Zarate, X.; Tomfohr, J.; Sankey, O. F.; Moore, A. L.; Moore, T. A.; Gust, D.; Harris, G.; Lindsay, S. M. *Science* **2001**, *294*, 571−574.
(7) Magoga, M.; Joachim, C. *Phys. Rev. B* **1997**, *56*, 4722−4729.
(8) Yaliraki, S. N.; Kemp, M.; Ratner, M. A. *J. Am. Chem. Soc.* **1999**, *121*, 3428−3434.
(9) Moresco, F.; Gross, L.; Alemani, M.; Rieder, K. H.; Tang, H.; Gourdon, A.; Joachim, C. *Phys. Rev. Lett.* **2003**, *91*, 036601(1−4).
(10) Reed, M. A.; Zhou, C.; Muller, C. J.; Burgin, T. P.; Tour, J. M. *Science* **1997**, *278*, 252−254.
(11) Reichert, J.; Ochs, R.; Beckmann, D.; Weber, H. B.; Mayor, M.; von Löhneysen, H. *Phys. Rev. Lett.* **2002**, *88*, 176804(1−4).
(12) Weber, H. B.; Reichert, J.; Weigend, F.; Ochs, R.; Beckmann, D.; Mayor, M.; Ahlrichs, R.; von Lohneysen, H. *Chem. Phys.* **2002**, *281*, 113−125.
(13) Smit, R. H. M.; Noat, Y.; Untiedt, C.; Lang, N. D.; van Hemert, M. C.; van Ruitenbeek, J. M. *Nature* **2002**, *419*, 906−909.
(14) Xu, B. Q.; Tao, N. J. J. *Science* **2003**, *301*, 1221−1223.
(15) He, J.; Chen, F.; Li, J.; Sankey, O. F.; Terazono, Y.; Herrero, C.; Gust, D.; Moore, T. A.; Moore, A. L.; Lindsay, S. M. *J. Am. Chem. Soc.* **2005**, *127*, 1384−1385.
(16) He, J.; Chen, F.; Liddell, P. A.; Andreasson, J.; Straight, S. D.; Gust, D.; Moore, T. A.; Moore, A. L.; Li, J.; Sankey, O. F.; Lindsay, S. M. *Nanotechnology* **2005**, *16*, 695−702.
(17) Chen, F.; He, J.; Nuckolls, C.; Roberts, T.; Klare, J. E.; Lindsay, S. *Nano Lett.* **2005**, *5*, 503−506.
(18) Haiss, W.; Van Zalinge, H.; Higgins, S. J.; Bethell, D.; Hobenreich, H.; Schiffrin, D. J.; Nichols, R. J. *J. Am. Chem. Soc.* **2003**, *125*, 15294−15295.
(19) Haiss, W.; Nichols, R. J.; van Zalinge, H.; Higgins, S. J.; Bethell, D.; Schiffrin, D. J. *Phys. Chem. Chem. Phys.* **2004**, *6*, 4330−4337.
(20) Xiao, X.; Xu, B.; Tao, N. *J. Am. Chem. Soc.* **2004**, *126*, 5370−5371.
(21) Xu, B. Q.; Zhang, P. M.; Li, X. L.; Tao, N. J. *Nano Lett.* **2004**, *4*, 1105−1108.
(22) Xiao, X. Y.; Xu, B. Q.; Tao, N. J. *Nano Lett.* **2004**, *4*, 267−271.
(23) Xu, B. Q.; Xiao, X. Y.; Yang, X. M.; Zang, L.; Tao, N. J. *J. Am. Chem. Soc.* **2005**, *127*, 2386-2387.
(24) Xiao, X. Y.; Nagahara, L. A.; Rawlett, A. M.; Tao, N. J. *J. Am. Chem. Soc.* **2005**, *127*, 9235−9240.

10.1021/ja057316x CCC: $33.50

site (e.g., on top or hollow sites) and the possibility of forming a thiol−Au rather than a thiolate−Au bond can significantly affect the measured conductance.[15,16,25−28]

We report here a study of the conduction mechanism of alkanedithiols and molecule−electrode contact effect on the conductance of the molecules using a combined STM and atomic force microscope (AFM) break junction method by varying various parameters. Although *N*-alkanedithiols (*N* is the number of methylene groups) have a rather large HOMO−LUMO gap and are considered to be "insulating", we chose the molecules as a model system for the following reasons. First, one can systematically study the length dependence of the conductance by varying *N*. Second, electron transfer through alkanethiol monolayers measured using different experimental techniques[29−36] all indicate that the conduction mechanism in these molecules is a tunneling or superexchange via the bond process. If the conduction mechanism of single alkanedithiols is also due to tunneling, then the conductance is described by $G = A \exp(-\beta_N N)$, where β_N is the decay constant and A describes the effect of the molecule−electrode contact. Because N can be varied systematically, one may gain insight into the molecule−electrode contact, described by the prefactor of the exponential function, A.

By performing the conductance measurement as a function of molecular length, temperature, in different solvents, and fitting of the current−bias voltage curves with models, we conclude that the conduction mechanism of single alkanedithiols covalently bound to two Au electrodes is dominated by tunneling via the C−C bonds along the alkane chains. The variation in the prefactor of the exponential function and simultaneous conductance and force measurements provide new insight into the effect of the molecule−electrode contact geometries on the conductance values of the molecules.

Experimental Method

The STM-break junction setup was a modified Pico-STM (Molecular Imaging) using a Nanoscope IIIa controller[24] or a Molecular Imaging controller. The Au STM tip was prepared by cutting a 0.25 mm gold wire (99.998%). The measurement of temperature dependence was performed using a high-temperature stage and Peltier stage (Molecular Imaging Corp.). The controllable temperature range of the setup was between −5 and 60 °C. The Teflon STM cell was cleaned with piranha solution and then sonicated in 18 MΩ water three times. (*Caution:* Piranha solution reacts violently with most organic materials and must be handled with extreme care.) The Au substrate was prepared by thermally evaporating 130 nm gold on mica in a UHV chamber.[37] Prior to each experiment, the substrate was briefly annealed in a hydrogen flame.

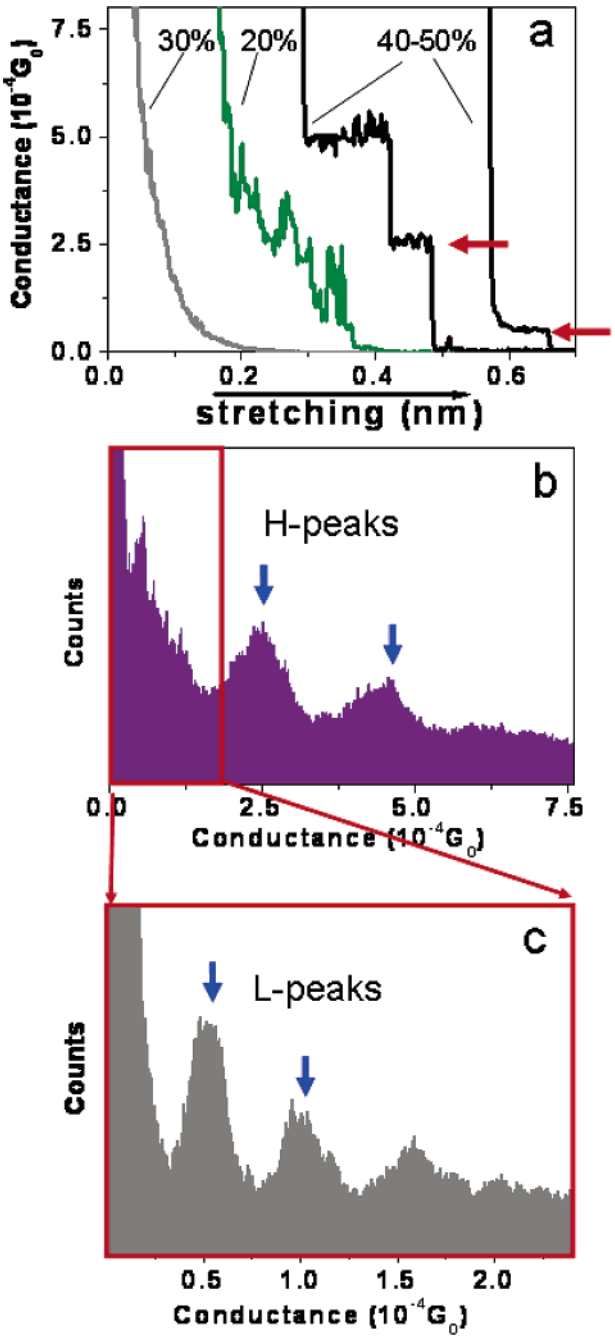

Figure 1. (a) Three types of transient conductance traces recorded during separation of the STM tip from the substrate in toluene containing 1 mM octanedithiol. The percentage frequency with which each occurs is marked on the graph. (b) Conductance histogram constructed from the conductance traces that show steps (486 out of 1193 curves). Peaks located near integer multiples are marked by arrows and referred to as H peaks. The region that shows spikes is marked by a rectangular box. (c) Conductance histogram of the rectangular box region reveals a new set of peaks (referred to as L peaks). Bias was 0.1 V in measurements. See text for details of the analysis.

The first step was to bring the STM tip within the tunneling distance to the substrate using the STM controller. The STM feedback was then turned off, and a separate computer was used to move the tip into and out of contact with the substrate at a typical rate of 20−40 nm/s. The transient conductance curves during the process were recorded with a digital oscilloscope. We observed three types of transient curves (Figure 1a). The first type is a smooth exponential decay due to electron

(25) Stokbro, K.; Taylor, J.; Brandbyge, M.; Mozos, J. L.; Ordejon, P. *Comput. Mater. Sci.* **2003**, *27*, 151−160.
(26) Emberly, E. G.; Kirczenow, G. *Phys. Rev. B* **1998**, *58*, 10911−10920.
(27) Kornilovitch, P. E.; Bratkovsky, A. M. *Phys. Rev. B* **2001**, *64*, 195413-(1−4).
(28) Tomfohr, J.; Sankey, O. F. *J. Chem. Phys.* **2004**, *120*, 1542−1554.
(29) York, R. L.; Nguyen, P. T.; Slowinski, K. *J. Am. Chem. Soc.* **2003**, *125*, 5948−5953.
(30) Holmlin, R. E.; Haag, R.; Chabinyc, M. L.; Ismagilov, R. F.; Cohen, A. E.; Terfort, A.; Rampi, M. A.; Whitesides, G. M. *J. Am. Chem. Soc.* **2001**, *123*, 5075−5085.
(31) Slowinski, K.; Chamberlain, R. V.; Miller, C. J.; Majda, M. *J. Am. Chem. Soc.* **1997**, *119*, 11910−11919.
(32) Wold, D. J.; Frisbie, C. D. *J. Am. Chem. Soc.* **2001**, *123*, 5549−5556.
(33) Chidsey, C. E. D. *Science* **1991**, *251*, 919−922.
(34) Smalley, J. F.; Feldberg, S. W.; Chidsey, C. E. D.; Linford, M. R.; Newton, M. D.; Liu, Y. P. *J. Phys. Chem.* **1995**, *99*, 13141−13149.
(35) Wang, W. Y.; Lee, T.; Reed, M. A. *Phys. Rev. B* **2003**, *68*, 035416(1−7).
(36) Wang, W. Y.; Lee, T.; Reed, M. A. *J. Phys. Chem. B* **2004**, *108*, 18398−18407.
(37) DeRose, J. A.; Thundat, T.; Nagahara, L. A.; Lindsay, S. M. *Surf. Sci.* **1991**, *256*, 102−108.

tunneling between the tip and the substrate. The percentage of these decay curves was 20−30% when performing the experiment in toluene containing ∼1 mM sample molecules. The exponential decay curves were usually rejected (either not recorded or removed after recording) in the construction of the conductance histogram because they would contribute a large background peak near zero current (or conductance). The second type of transient curve was noisy and rapidly varying, probably due to mechanical vibrations, acoustic noise, and impurities in the sample cell. The percentage of the noisy curves was around 20−30%, and they were also rejected when constructing the conductance histogram. The remaining 40−50% were curves with clear steps, which were used to construct the conductance histogram. The conductance histograms are constructed by counting the number of times each step occurs and weighting that number by the time duration of the step.

To determine the possible effect of the sample preparation on the measured conductance, we have performed the measurements using two different sample preparation procedures. The first one is to measure the conductance in a solvent containing 1 mM alkanedithiols so that the molecules can adsorb on both the tip and the substrate electrodes during the measurement. The second one is to pre-assemble a monolayer of alkanedithiol on Au substrate by exposing the substrate to 1 mM alkanedithiol solution overnight. This is known to lead to a rather compact coverage of the alkanedithiols on Au electrodes. The conductance measurement was then performed using the substrate in a solvent containing no alkanedithiol molecules. The second approach has a lower yield of conductance curves with stepwise features.

Similar to the STM break junction experiment described above, we performed the measurement using a conducting AFM break junction to record the force and conductance simultaneously during the breakdown of individual molecular junctions. The AFM tip was made of Si (Nanoscience Instruments) coated with 20 nm layer of chromium and then 50 nm layer of gold (99.999%) using an ion beam coater (Gatan model 151) before each measurement. The spring constant of the AFM cantilever was calibrated to be 36 N/m.

Results and Discussion

Statistical Analysis of Repeatedly Formed Molecular Junctions. Figure 1b is a conductance histogram of octanedithiol. Pronounced peaks marked by arrows are located at integer multiples of 2.5×10^{-4} G_0, where $G_0 = 2e^2/h \approx 77.5$ μS. This result is in good agreement with the previously reported conductance by Xu et al.[14] In addition to the pronounced peaks, the histogram also shows spike-like features between the origin and the first conductance peak. Carefully examining the region of the spike-like feature reveals a new set of peaks located at integer multiples of $\sim 0.52 \times 10^{-4}$ G_0, which is about 5 times lower in conductance (Figure 1c). We refer to the two sets of conductance peaks as H (high conductance) and L (low conductance) peaks. Haiss et al. have reported two sets of steps in their conductance measurements; one set has conductance close to 2.5×10^{-4} G_0.[19] From the histograms that show both the H and the L peaks, we determined that the probability of finding the H peaks is about 2−2.5 times greater than that of the L peaks. In certain conditions, we also saw features corresponding to much lower conductivity (see discussion below).

Control Experiments. We repeated the measurement using STM- and AFM-break junctions, different current amplifiers, and also in different labs, reproducing the key findings in every experiment. To check for the effects of oxidation or degradation of the sample molecules, we confirmed the observations using both old and freshly prepared samples. We also performed the experiments in a sealed, oxygen free system coupled to a glovebox. Additionally, we carried out control experiments by performing the same measurements in pure toluene, in toluene containing 1 mM ω-octanemonothiol, in pure water, in dodecane, and in 0.1 M $NaClO_4$. In the case of toluene, 98.7% (810 curves) of 836 curves are smooth exponential decays (Figure 2a). The rest 1.3% of the curves show some kinks or steplike features (Figure 2b), which are random, and the corresponding histogram exhibits no obvious peaks. We attribute these features to impurities and mechanical vibrations. In the presence of monothiols, the percentage of featureless exponential decay curves is 99.7% (828 out of 836 curves), and the percentage of curves with some features is only 0.3%. The control experiment with monothiols not only provides further evidence that the peaks in the conductance histograms are due to the molecules, but also shows that the presence of thiols at both ends of the molecules are necessary to form well-defined molecular junctions.

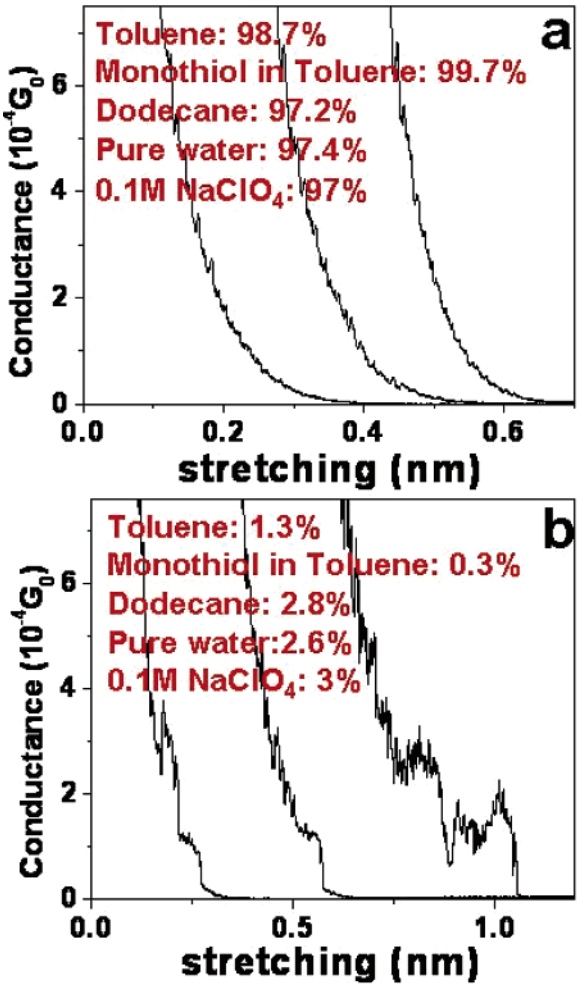

Figure 2. Control experiments in pure toluene, in toluene containing 1 mM octanemonothiol, in dodecane, in pure water, and in 0.1 M $NaClO_4$. The vast majority of the conductance traces are smooth exponential decays (a), and a small number of traces show kinks and steplike features (b). Bias was 0.1 V in the measurements.

Solvent Effects. We have performed most of our measurements in a solvent for two reasons because it reduces contaminations from ambient environment, and it facilitates introduction of sample molecules. However, the use of solvent raises several questions: Does electron tunneling through the solvent contribute significantly to measured conductance of the molecules?

Table 1. Conductance Values of Both H- and L-Sets of Octanedithiol in Different Solvents[a]

solvent	H-conductance (10^{-4} G_0)	L-conductance (10^{-4} G_0)
toluene	2.5 ± 0.5	0.5 ± 0.1
dodecane	2.5 ± 0.5	0.5 ± 0.1
pure water	2.5 ± 0.5	0.5 ± 0.1
0.1 M $NaClO_4$	2.5 ± 0.5	0.5 ± 0.1

[a] Bias was 0.1 V in all of the measurements in this table.

If the solvent does not directly contribute to the measured conductance, does it change the conductance of the molecules via interactions with the molecules? To answer these questions, we have performed the conductance measurement of alkanedithiol in polar, ionic, and nonpolar solvents, including pure water, 0.1 M $NaClO_4$, toluene, and dodecane. We have observed both H and L sets of the conductance peaks in all of the solvents, and the conductance values are identical in all of the solvents within the experimental uncertainties (Table 1). This observation shows that tunneling via the solvent molecules does not contribute significantly to the measured conductance, and they do not affect the conductance of alkanedithiols either.

Temperature Effect. Many of the reported works strongly suggest that the conduction mechanism in alkanes is dominated by a coherent tunneling or superexchange process, for which the simple tunneling model predicts a temperature-independent conductance. Reed et al. have studied alkanethiol self-assembled monolayers sandwiched between two Au electrodes and observed that the conduction through the monolayers is independent of temperature, thus providing strong evidence of tunneling as the conduction mechanism in the molecular assembly. We have measured conductance of alkanedithiol as a function of temperature. Within the temperature window that is available in our current setup and experimental error bars, both the H- and the L-conductance values of the molecules are independent of temperature (see Figure 3). If assuming that the conduction still involves some thermally activated processes, then the maximum activation energies estimated from the error bars are 0.03 eV, same for the H- and L-conductance values.

Current−Voltage Curves. Different conduction mechanisms may be reflected in characteristic shapes of the current versus bias voltage ($I-V$) curves. For example, thermionic emission predicts $I \approx \exp(V^{1/2})$, while the simple tunneling process predicts a linear dependence of I on V for small V. A more explicit $I-V$ relation has been worked by Simmons,[38] which expressed the tunneling current through a barrier in the tunneling regime of $eV < \phi_B$, where ϕ_B is the barrier height, as

$$I \propto (\phi_B - eV/2)\exp\left[-\frac{2(2m)^{1/2}}{\hbar}\alpha(\phi_B - eV/2)^{1/2}L\right] - (\phi_B + eV/2)\exp\left[-\frac{2(2m)^{1/2}}{\hbar}\alpha(\phi_B + eV/2)^{1/2}L\right] \quad (1)$$

where m is the electron mass, L is the barrier width, and α is an adjustable parameter to account for nonideal tunneling barrier and the effective mass of the tunneling electrons.[7,30,35,39]

We have measured $I-V$ curves of octanedithiols using two approaches. The first one is to monitor the peak positions in the conductance histograms obtained at different bias voltages.

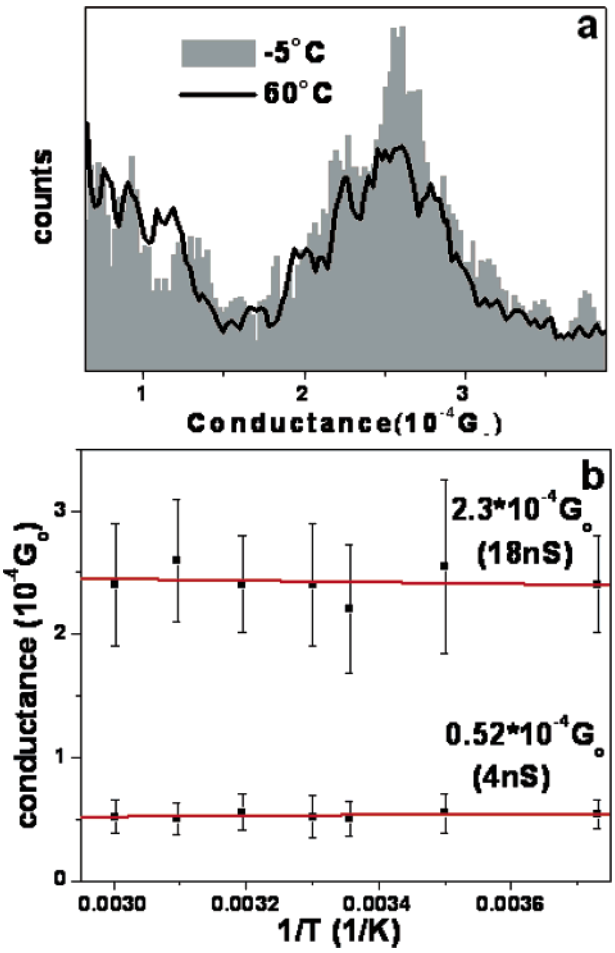

Figure 3. (a) Conductance histograms of octanedithiol at −5 and 60 °C showing temperature independence for the H-peaks. (b) Conductance values of the H- and L-sets versus temperature. Bias was 0.1 V in the measurements.

The second one is to pull the tip until the lowest conductance plateau (corresponding to the formation of a single molecular junction) is reached. The electrodes are then fixed in position, and the current through the molecule is recorded as a function of the bias voltage. The two methods give consistent results as shown in Figure 4a. The $I-V$ curves are linear for $V < 0.5$ V and become nonlinear for $V > 0.5$ V. It is interesting to note that dividing the $I-V$ curves of the H-conductance by 5 produces curves that are indistinguishable from those of the L-conductance. We have performed nonlinear-least-squares fitting of the measured $I-V$ curves for both L- and H-conductance values using the Simmons model. Reasonable fits to the data can be obtained with a range of fitting parameters, α and Φ_B (listed in Figure 4b). However, these parameter values all yield the same value for the corresponding decay constant $\beta = \alpha\Phi_B^{1/2} \approx 0.8$ Å^{-1}.

Length Dependence. Another important signature of the tunneling mechanism is exponential decrease of the conductance on the molecular length. We measured the conductance of two other dithiols, hexanedithiol and decanedithiol, to study the dependence of the conductance on the molecular length. Two sets of peaks also appeared in the conductance histograms of these molecules. Logarithmic plots of the conductance versus molecular length (N) show that both the L- and the H-conductance values follow the simple tunneling model given

(38) Simmons, J. G. *J. Appl. Phys.* **1963**, *34*, 1793−1803.
(39) Tomfohr, J. K.; Sankey, O. F. *Phys. Rev. B* **2002**, *65*, 245105(1−12).

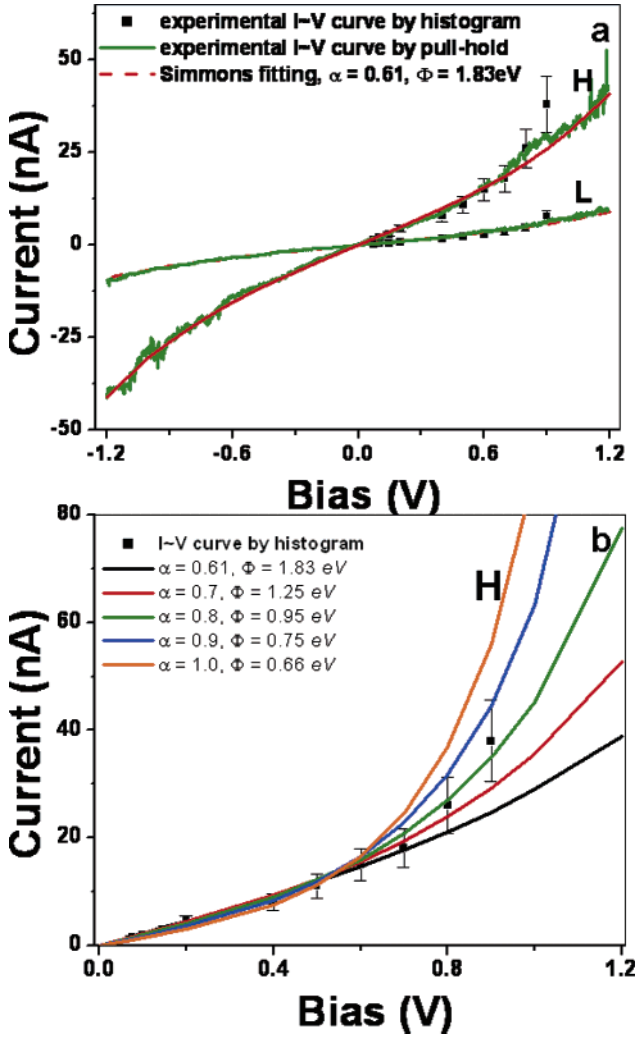

Figure 4. (a) Experimental $I-V$ curves of octanedithiol for both L- and H-conductance values obtained from single bias sweep (green solid lines) and from the positions of the peaks in the conductance histograms (■). Fitting to the Simmons model with $\alpha = 0.61$ and $\Phi_B = 1.83$ eV is given by red lines. (b) Sensitivity of the fitting to the fitting parameters α and Φ_B.

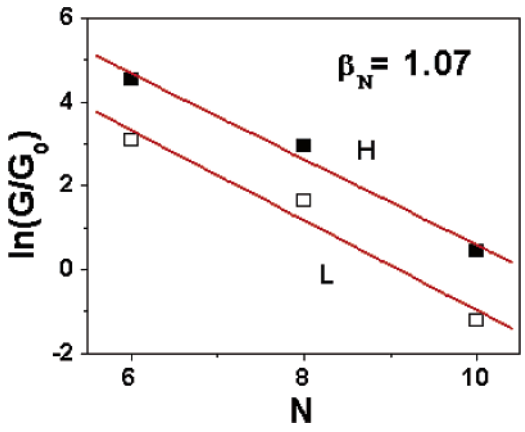

Figure 5. Natural logarithm of conductance versus N (number of carbon atoms in the N-alkanedithiols) for both the H (■) and the L (□) peaks. The solid lines are linear fits that yield β_N.

by $G = A \exp(-\beta_N N)$ (Figure 5). The systematic dependence of the conductance on the molecular length confirms that both sets of peaks are due to conductance of alkanedithiols. The exponential decay also allows us to rule out the possible assignment of the L conductance to the formation of dimers (two alkanedithiols are bound via S−S bonds between them). This is because a dimer would be twice the length of a monomer, and its conductance would be several orders of magnitude smaller than the monomers, rather than a factor of 4−5 observed for the L-conductance set.

From the slopes of the logarithmic plot, we found that the decay constants of both the L- and the H-conductance values are $\beta_N = 1.07 \pm 0.05$ (or ~ 0.85 Å^{-1}), which are consistent with the fitting of the $I-V$ curves to the Simmons model. These β values are also in good agreement with the widely accepted value in the literature for electron transfer through alkanethiol monolayers using nanopores,[35] mercury contacts,[29−31] and with coupling to a redox group.[33,34] The difference between the L- and H-conductance molecular junctions is contained in the prefactor of the exponential function, A, which is about 0.7 for the H and 0.14 for the L sets. Because A describes the molecule−electrode contact, we attribute two types of molecular junctions to two different molecule−electrode contact geometries.

Measurement of Molecule−Electrode Breakdown Forces. To learn more about the origin of the two sets of peaks, we performed the measurements using conducting AFM to determine simultaneously the conductance and the force associated with the breakdown of the conductance steps. Figure 6a and b plots both force and conductance curves obtained during the breakdown processes of octanedithiol junctions. The conductance curve (Figure 6b) shows both the H and the L steps, and the H step is approximately 5 times higher than that of the L step as found in the STM-break junction measurement. Associated with each abrupt step (H or L) in the conductance is a drop in the force, which provides a measurement of the breakdown force. Although the conductance histogram clearly reveals the same H and L peaks as seen in the STM, the force histograms shows that the average breakdown forces for both H and L steps are the same (only one peak at about 1.5 nN) (Figure 6d). Because the average force required to break a Au−Au bond measured under the same condition is also ~1.5 nN, we believe that the breakdown of the molecular junctions takes place at the Au−Au bond; that is, a Au atom is pulled out of the Au electrode and attached to S after the breakdown.[40] More importantly, the simultaneous force and conductance measurement shows that the breakdown of H and L molecular junctions involves similar chemical bindings. This observation rules out the possible coexistence of molecular junctions involving both thiolate−Au and thiol−Au bonds because the thiol−Au bond would break at a smaller force.

Origin of the Multiple Steps. To gain further insights into the microscopic nature of the molecule−electrode contact geometries that lead to the two sets of conductance values, we have studied statistical correlations between the occurrences of the H and L conductance steps. Any one conductance curve (cf., Figure 1a) generally only has H or L steps (but rarely both). When both are observed in the same curve, then it is always as an L step occurring right after an H step (Figure 6b). We have never observed an H step occurring after an L step. On the basis of these observations, we propose the following model. The H step corresponds to a molecule with one end (S) sitting on a

(40) Xu, B. Q.; Xiao, X. Y.; Tao, N. J. *J. Am. Chem. Soc.* **2003**, *125*, 16164−16165.

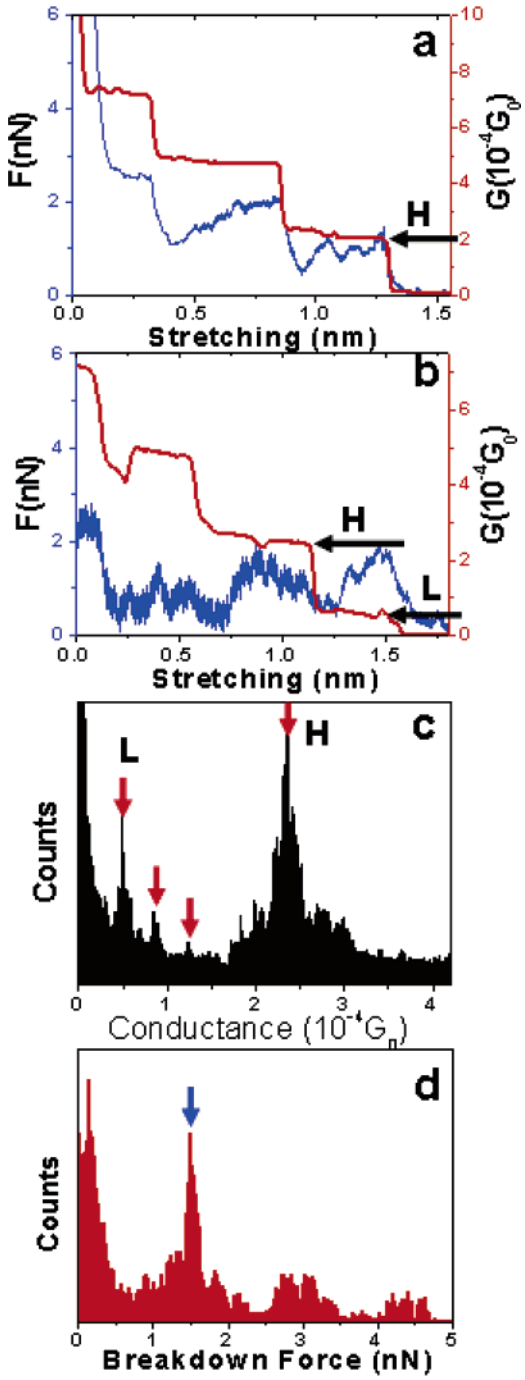

Figure 6. (a) Conductance and force traces showing H steps only. (b) Conductance and force traces showing H steps followed by L steps. (c) Conductance histogram reveals both H and L peaks. (d) Force histogram constructed from 220 force traces (recorded simultaneously with current acquisition) shows that both H and L have the same breakdown force. The measurements were performed in toluene containing 1 mM octanedithiol, and bias was 0.1 V.

hollow site of a Au electrode and the other end on a top site of the second Au electrode, or a top-hollow geometry (Figure 7). The L molecule junction is the case where both ends sit on top sites, or a top-top geometry (Figure 7). This model explains all of the observed facts. First, the breakdown forces are the same for both the H and the L junctions because they both pull a Au atom out of the electrode from the molecule-top binding site. Second, the occurrence of the H junctions is about twice as likely as that of the L junctions, which can be attributed to the

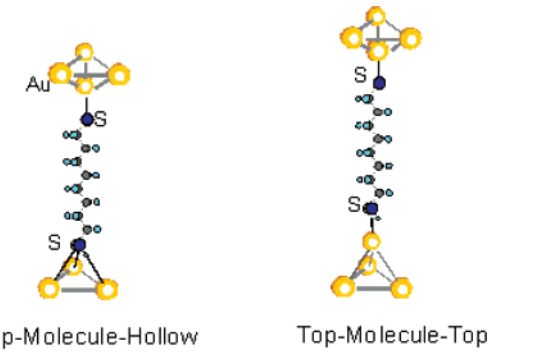

Figure 7. Models of two different molecule−electrode contact geometries.

fact that the top-hollow geometry should be twice as frequent as the top-top geometry. Finally, an L step can occur after an H step, but it never occurs before the H step. This is because under a tensile force it is unlikely for a contact to change from the molecule-top binding geometry to molecule-hollow geometry. Simulations suggest that the difference between top-top and hollow-hollow connected molecules is not large (at least for the special case of octanedithiol). However, more recent simulations of a connection to a pyramidal site (e.g., attachment to a Au atom sitting on top of a three-fold hollow) do show ca. a 4-fold decrease in conductance (O. F. Sankey, unpublished), consistent with the discussion above.

The remaining question is why hollow-hollow geometry does not occur or else occurs with a small probability. This may be explained by the way that each molecular junction is formed in the present experiments. We form a molecular junction by pulling two electrodes apart, and the signature of the formation of molecular junction is a step in the conductance transient curve. To observe the step, one has to stretch the molecular junction over a finite distance, which occurs primarily by pulling gold atoms out of the electrodes and leads to an on-top geometry at least at one of the two contacts. Other possibilities involving binding to the bridge site may have low probabilities and be buried in the noise of the conductance histograms.

Thermally Activated Feature. Haiss has measured the conductance of alkanedithiols by trapping the molecules between a STM tip and a Au substrate and reported a conductance several times smaller than the L-conductance observed here. More recently, they have found that the conductance is sensitive to temperature and scales logarithmically with $1/T$, where T is temperature. We have searched for such features using our approaches and did not found pronounced peaks in the conductance histograms using the two sample preparation procedures described in the experimental section. However, when we decrease the coverage of the alkanedithiols by reducing the exposure time of the substrate to the molecules, a feature similar to that reported by Haiss et al. appears. The temperature dependence indicates that the origin of the feature is a thermally activated process, but the mechanism of the process needs further studies. Intriguingly, this feature shares many properties with the conductance reported for a single molecule connected by means of a gold nanoparticle.[6] The low bias conductance is identical (1 nS), the electronic decay constant is anomalous and

has the same value in both cases (ca. 0.6 per added methylene),[6] and the current voltage curve has an anomalously large linear region.[41]

Summary

We have determined the conductance of single *N*-alkanedithiols ($N = 6$, 8, and 10) covalently connected to two gold electrodes by repeatedly creating many gold−molecule−gold junctions using a combined STM- and AFM-break junction approach. For each molecule, the conductance histogram constructed from the repeated measurements reveals two sets of well-defined peaks at integer multiples of two fundamental conductance values. The ones with higher conductance agree with what has been reported previously. The lower ones occur 2−2.5 times less frequently and have a conductance 4−5 times smaller. Both the high and the low conductance values are independent of temperature within experimentally accessible range and errors. They are also similar in several different solvents. Both conductance values decay exponentially with the length of the molecule with a decay constant of 0.84 $Å^{-1}$. The $I-V$ curves of the high and low conductance values can be fit with the Simmons tunneling model. The forces required to break both types of molecular junctions are the same, which is 1.5 nN. These observations lead us to believe that both are due to electron tunneling or superexchange via the bonds along the molecules but with two different molecule−electrode contact geometries. This work suggests that the conductance of a single molecule is sensitive to the microscopic details of the contacts. It also shows that although the STM break junction, together with statistical analysis, can provide reproducible data, variations in the molecule−electrode contact geometry can lead to more than one result for the conductance of single molecule.

Acknowledgment. We thank Otto Sankey and Thomas Wandlowski for discussions and the NSF (CHE-0243423 and ECS 01101175) for financial support.

JA057316X

(41) Tomfohr, J.; Ramachandran, G.; Sankey, O. F.; Lindsay, S. M. *Making contacts to single molecules: Are we nearly there yet?*; Springer: Berlin, 2005.